



SAND2007-1593C

SAND2007-xxxxC

# Concrete Fracture and Failure Modeling with Peridynamics

---

Stewart Silling

Paul Demmie

John Foster

Sandia National Laboratories

Walter Gerstle  
University of New Mexico

Thomas Warren  
Consultant

*Workshop on Modeling Concrete Under High Impulsive Loadings, Austin, TX*  
March 21, 2007

Sandia is a multiprogram laboratory operated by Sandia Corporation, a Lockheed Martin Company, for the United States Department of Energy's National Nuclear Security Administration under contract DE-AC04-94AL85000.



## Outline

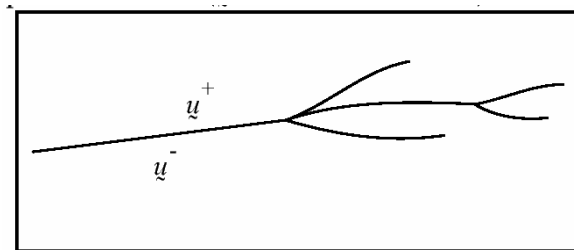
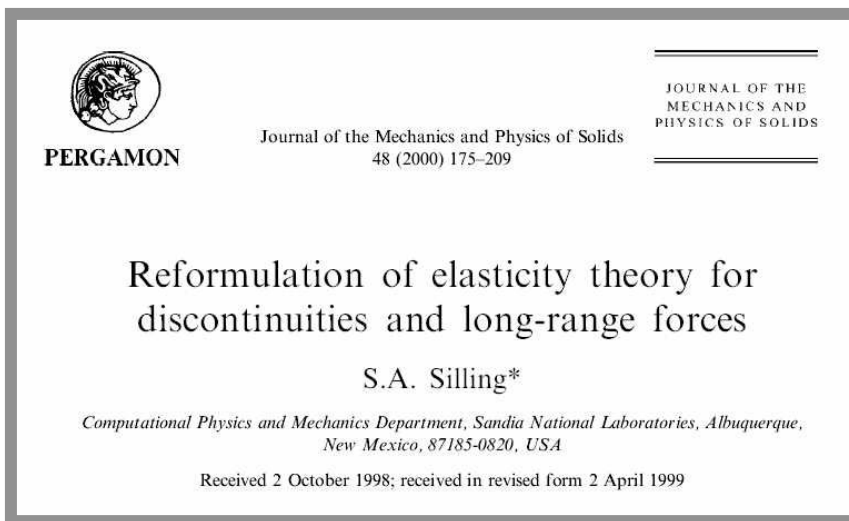
---

- Theory
  - What makes this different?
- Single crack growth
- Concrete applications
  - Perforation
    - Single panel: effect of impact angle
    - Multiple panels
    - Effect of reinforcement
  - Damage accumulation due to multiple impacts
  - Fragmentation and fragment distribution
  - Blast loading
  - Deep penetration
    - Target size effect



# Peridynamic theory: What makes this different

- Why is it so hard to model fracture with conventional finite element codes?
  - The fundamental PDEs do not apply on a crack.
- New approach: peridynamic theory uses integral rather than differential equations.
  - Reformulation of the fundamental equations.
  - Equations apply everywhere regardless of discontinuities.
  - No need for externally supplied “crack growth law”.
  - Cracks initiate, grow spontaneously.
  - Theory first published in 2000:



Real life:  
Discontinuities can evolve in complex  
patterns not known in advance.



## Peridynamic theory: basic equations

---

Classical theory:

$$\rho \ddot{u}(\underline{x}, t) = \nabla \bullet \underline{\sigma}(\underline{x}, t) + \underline{b}(\underline{x}, t)$$

where  $\rho$  = density,  $\underline{u}$  = displacement,  $\underline{\sigma}$  = stress tensor field, and  $\underline{b}$  = body force field.

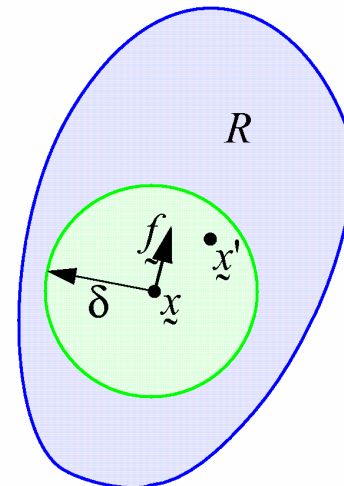
Peridynamic theory:

$$\rho \ddot{u}(\underline{x}, t) = \underline{L}_u(\underline{x}, t) + \underline{b}(\underline{x}, t)$$

where

$$\underline{L}_u(\underline{x}, t) = \int_R f(\underline{u}(\underline{x}', t) - \underline{u}(\underline{x}, t), \underline{x}' - \underline{x}) dV_{\underline{x}'}$$

and  $f$  is a vector-valued function.

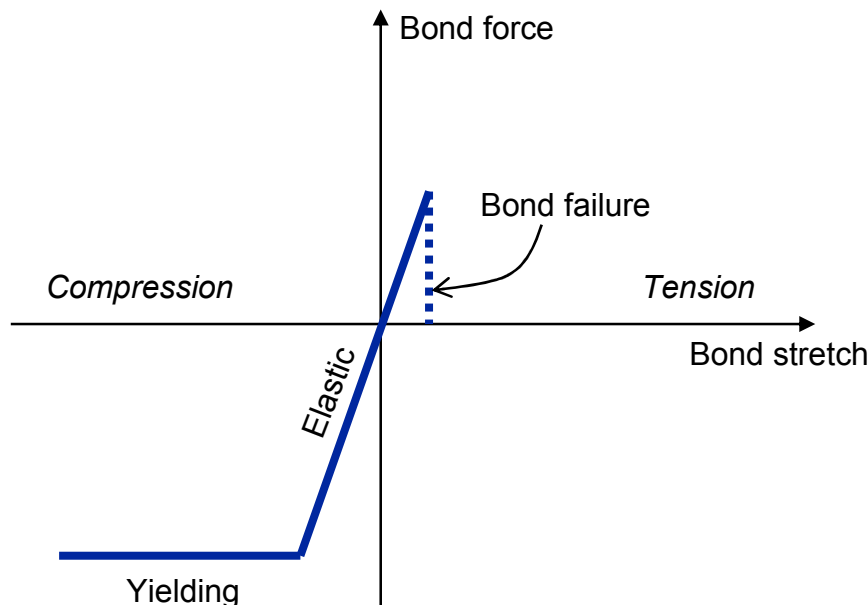




## Peridynamic theory: Material model

---

- All material-specific behavior is contained in the function  $f$ .
- Material parameters come from measurable elastic-plastic and fracture data.





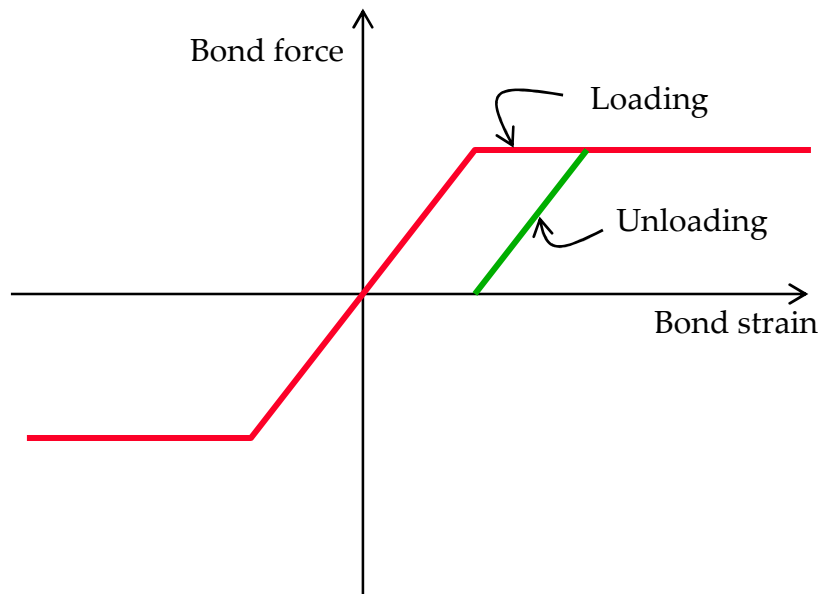
## Peridynamic theory: Other constitutive models

---

- Visco-microelastic:

bond force =  $f(r, \dot{r}, \xi)$ ,  $r = |\xi + \eta|$  = current distance between  $x$  and  $x'$

- Microplastic:

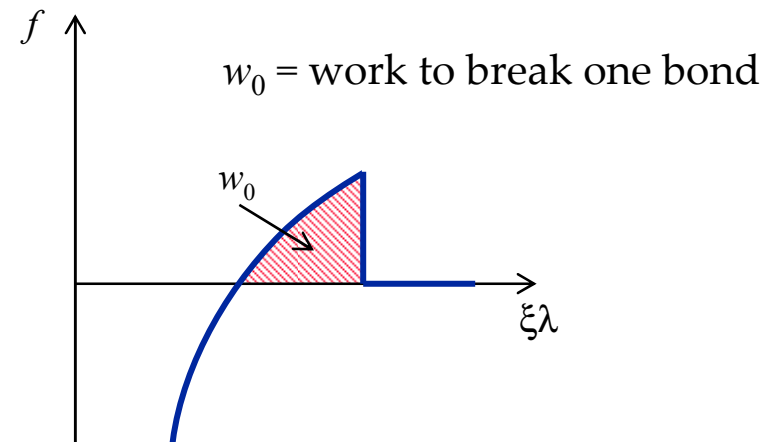
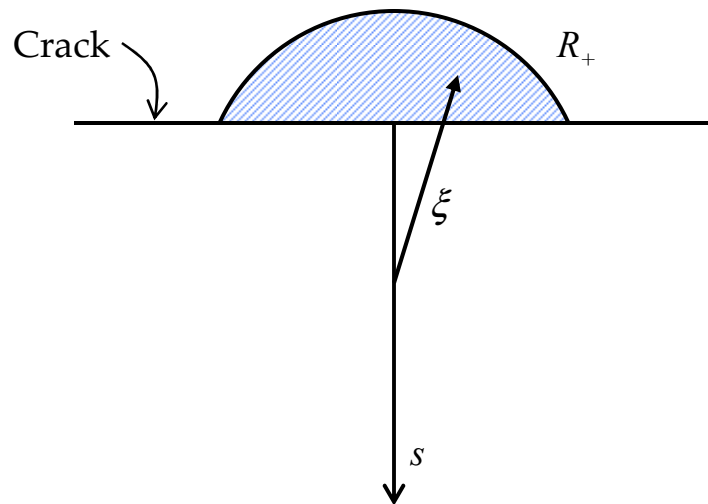




## Peridynamic theory: Energy required to advance a crack

- Adding up the work needed to break all bonds across a line yields the energy release rate:

$$G = 2h \int_0^\delta \int_{R_+} w_0 dV ds$$



There is also a version of the J-integral that applies in this theory.

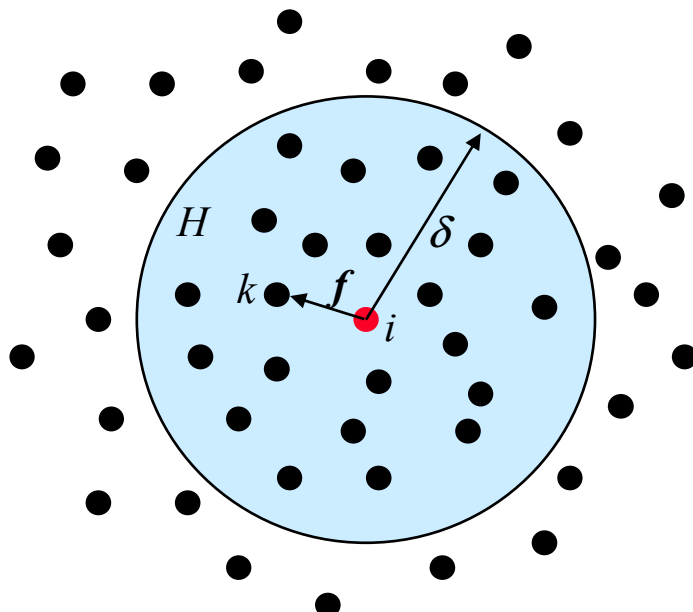


## EMU numerical method

---

- Integral is replaced by a finite sum.
- The resulting method is meshless and Lagrangian.

$$\rho \ddot{\mathbf{u}}_i^n = \sum_{k \in H} f(\mathbf{u}_k^n - \mathbf{u}_i^n, \mathbf{x}_k - \mathbf{x}_i) \Delta V_i + \mathbf{b}(\mathbf{x}_i, t)$$

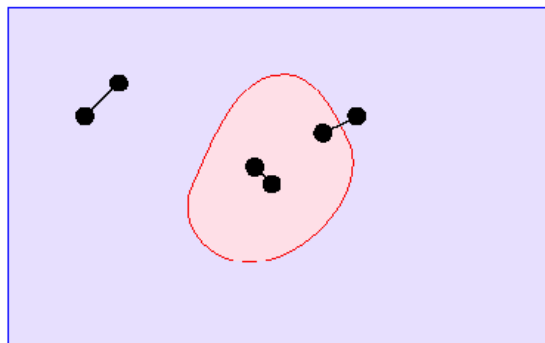




## EMU numerical method: Code features

---

- Meshfree (no elements)
- Lagrangian (each node represents a fixed amount of material)
- Parallel (runs on multiple processors)
- Explicit (simple, reliable time integration method)
- “Unguided” crack growth.
  - No need for an externally supplied crack growth law for:
    - Initiation, growth velocity, direction, branching, arrest, . . .
  - Any number of cracks can occur spontaneously.
  - Interface bonds are treated the same as other bonds.





## EMU numerical method: Relation to SPH

SPH

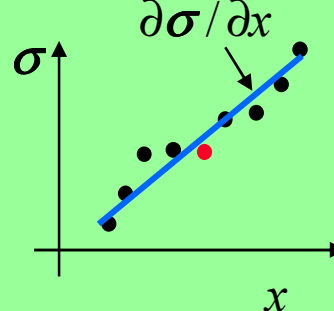
$$\frac{\partial v}{\partial x} = \int v(x') K(x') dV'$$

$$\dot{\varepsilon} = \frac{1}{2} \left( \left( \frac{\partial v}{\partial x} \right) + \left( \frac{\partial v}{\partial x} \right)^T \right)$$

$$\sigma = \sigma(\varepsilon)$$

$$\frac{\partial \sigma}{\partial x} = \int \sigma(x') K(x') dV'$$

$$\rho \ddot{u} = \frac{\partial \sigma}{\partial x} + b$$



- Both are meshless Lagrangian methods.
- Both involve integrals.
- But the basic equations are fundamentally different:
  - SPH relies on curve fitting to approximate derivatives that appear in the classical PDEs.
  - Peridynamics does not use these PDEs, relies on pair interactions.

Emu

$$\rho \ddot{u}(x) = \int f(u(x') - u(x), x' - x) dV' + b(x)$$





## Discretized model: Relation to finite elements

---

- Can solve the peridynamic equations in a framework similar to FE.
- Can include rotational degrees of freedom, leads to a micropolar model.
- Typical element stiffness matrix (for truss-like element)\*:

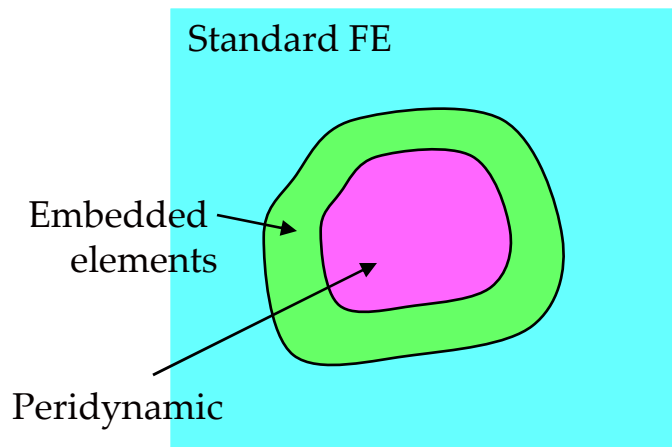
$$\begin{bmatrix}
 \hat{f}_{jix} \\
 \hat{f}_{jiy} \\
 \hat{f}_{jiz} \\
 \hat{m}_{jix} \\
 \hat{m}_{jiy} \\
 \hat{m}_{jiz} \\
 \hat{f}_{ijx} \\
 \hat{f}_{ijy} \\
 \hat{f}_{ijz} \\
 \hat{m}_{ijx} \\
 \hat{m}_{ijy} \\
 \hat{m}_{ijz}
 \end{bmatrix} = \begin{bmatrix}
 \frac{E' A}{L} & & & & & & & & \\
 & \frac{12E'I}{L^3} & & & & & & & \\
 0 & & \frac{12E'I}{L^3} & & & & & & \\
 0 & 0 & & \frac{E'J}{L} & & & & & \\
 0 & 0 & 0 & & \frac{4E'I}{L} & & & & \\
 0 & 0 & \frac{-6E'I}{L^2} & 0 & 0 & \frac{4E'I}{L} & & & \\
 0 & \frac{-6E'I}{L^2} & 0 & 0 & 0 & & \frac{E' A}{L} & & \\
 \frac{-E' A}{L} & 0 & 0 & 0 & 0 & & & \frac{12E'I}{L^3} & \\
 0 & \frac{-12E'I}{L^3} & 0 & 0 & 0 & -\frac{6E'I}{L^2} & 0 & & \\
 0 & 0 & \frac{-12E'I}{L^3} & 0 & \frac{6E'I}{L^2} & 0 & 0 & \frac{12E'I}{L^3} & \\
 0 & 0 & 0 & \frac{-E'J}{L} & 0 & 0 & 0 & 0 & \frac{E'J}{L} \\
 0 & 0 & \frac{-6E'I}{L^2} & 0 & \frac{2E'I}{L} & 0 & 0 & \frac{6E'I}{L^2} & 0 & \frac{4E'I}{L} \\
 0 & \frac{6E'I}{L^2} & 0 & 0 & 0 & \frac{2E'I}{L} & 0 & -\frac{6E'I}{L^2} & 0 & 0 & \frac{4E'I}{L}
 \end{bmatrix} \begin{matrix} (sym) \\ \left. \begin{array}{c} \hat{u}_i \\ \hat{v}_i \\ \hat{w}_i \\ \hat{\theta}_{xi} \\ \hat{\theta}_{yi} \\ \hat{\theta}_{zi} \\ \hat{u}_j \\ \hat{v}_j \\ \hat{w}_j \\ \hat{\theta}_{xj} \\ \hat{\theta}_{yj} \\ \hat{\theta}_{zj} \end{array} \right\} \end{matrix}$$

\* W. Gerstle et. al., to appear in *Nuclear Engineering & Design* (2007).

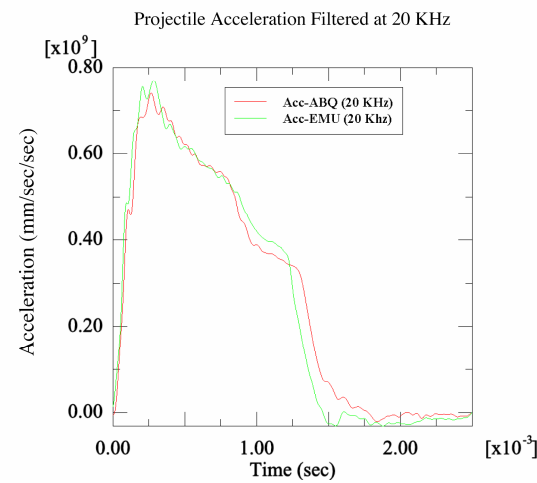
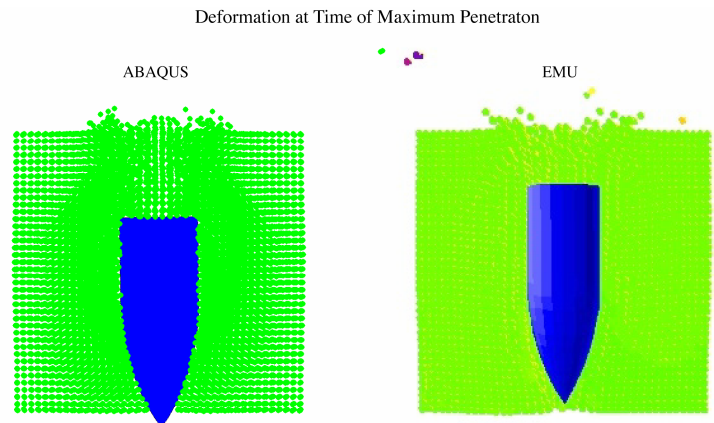


## Relation to finite elements: ABAQUS implementation

- The Emu peridynamic solution method has been implemented in a special version of ABAQUS\*.
- Can interface peridynamic elements with conventional FE by using embedded elements.



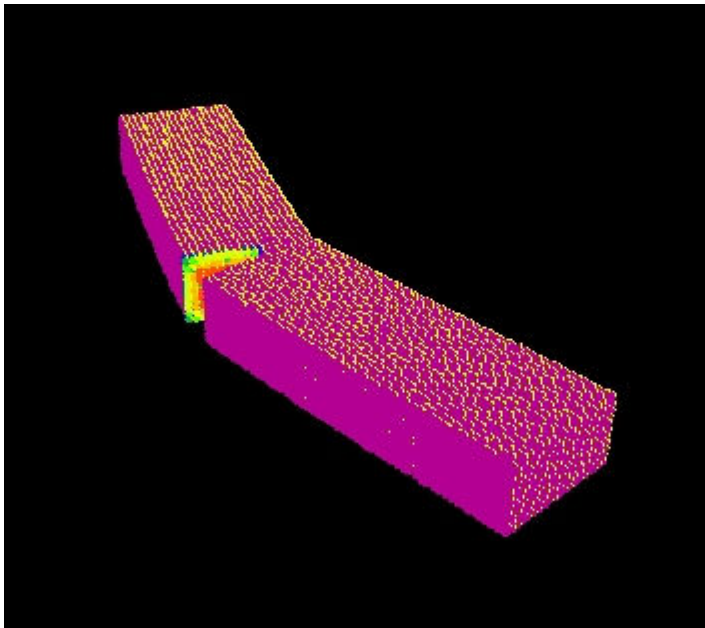
\* R. Macek, LANL Report LA-14300, July 2006 .



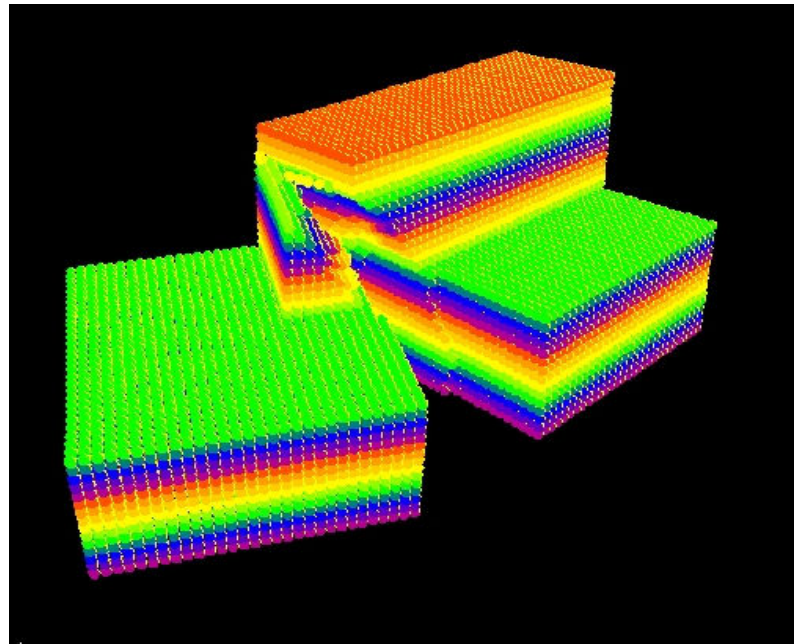


## Single crack growth in metals: Examples

---



3-point bend



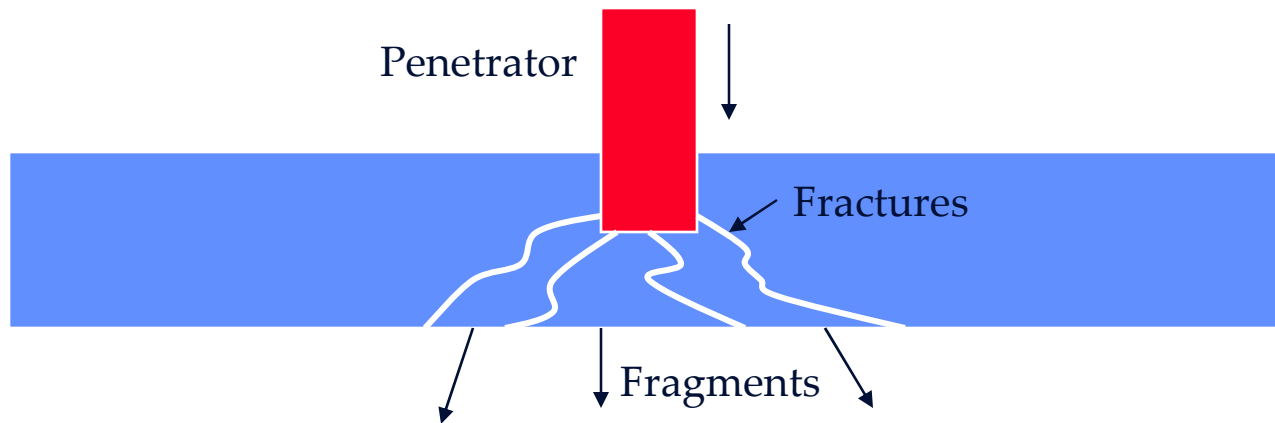
A more complex geometry



## Perforation: Why use this method?

---

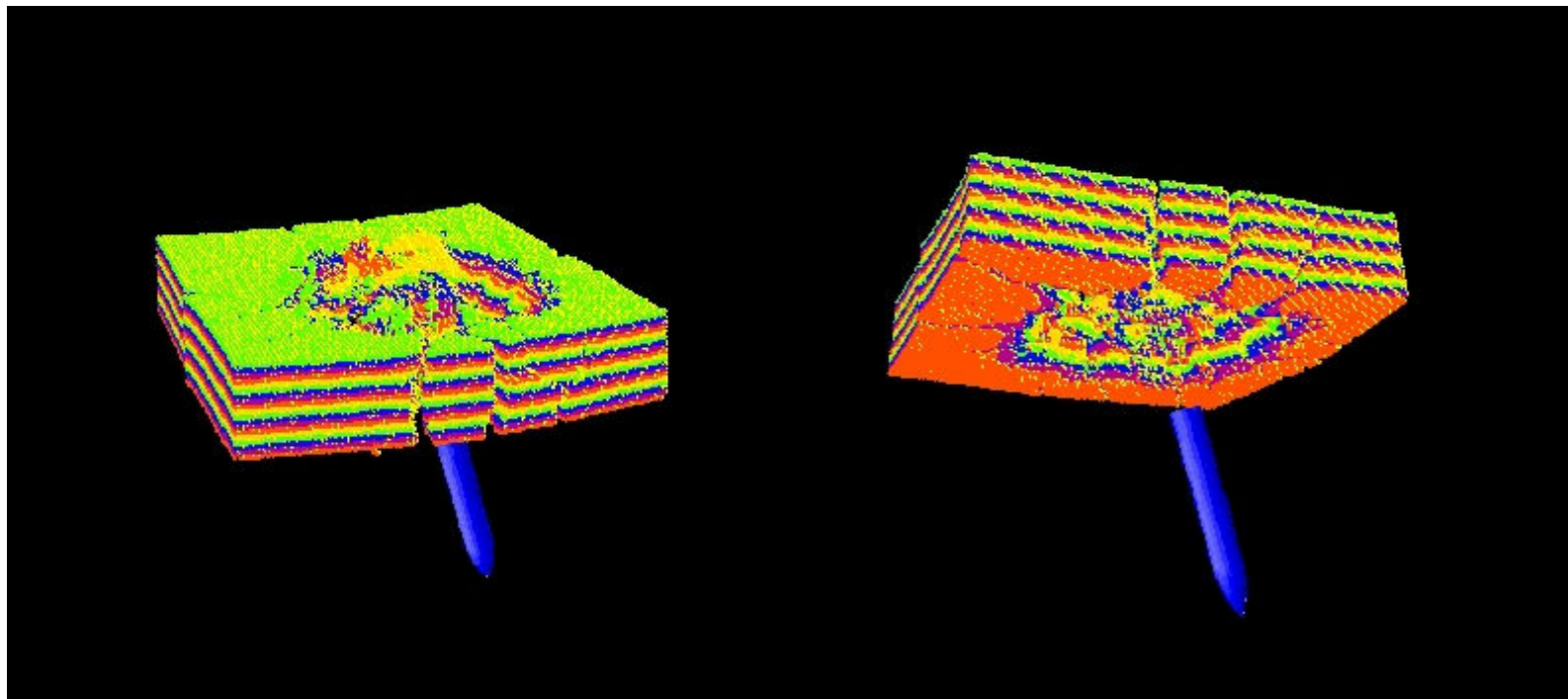
- Ability to model fracture is important for perforation.
  - Target starts weakening long before the penetrator gets through.
  - Fracture growth process determines fragment properties.





## Perforation: Typical results

- Cratering has some effect on the acceleration.
  - Weakening in the exit crater “attracts” the nose (more discussion later).



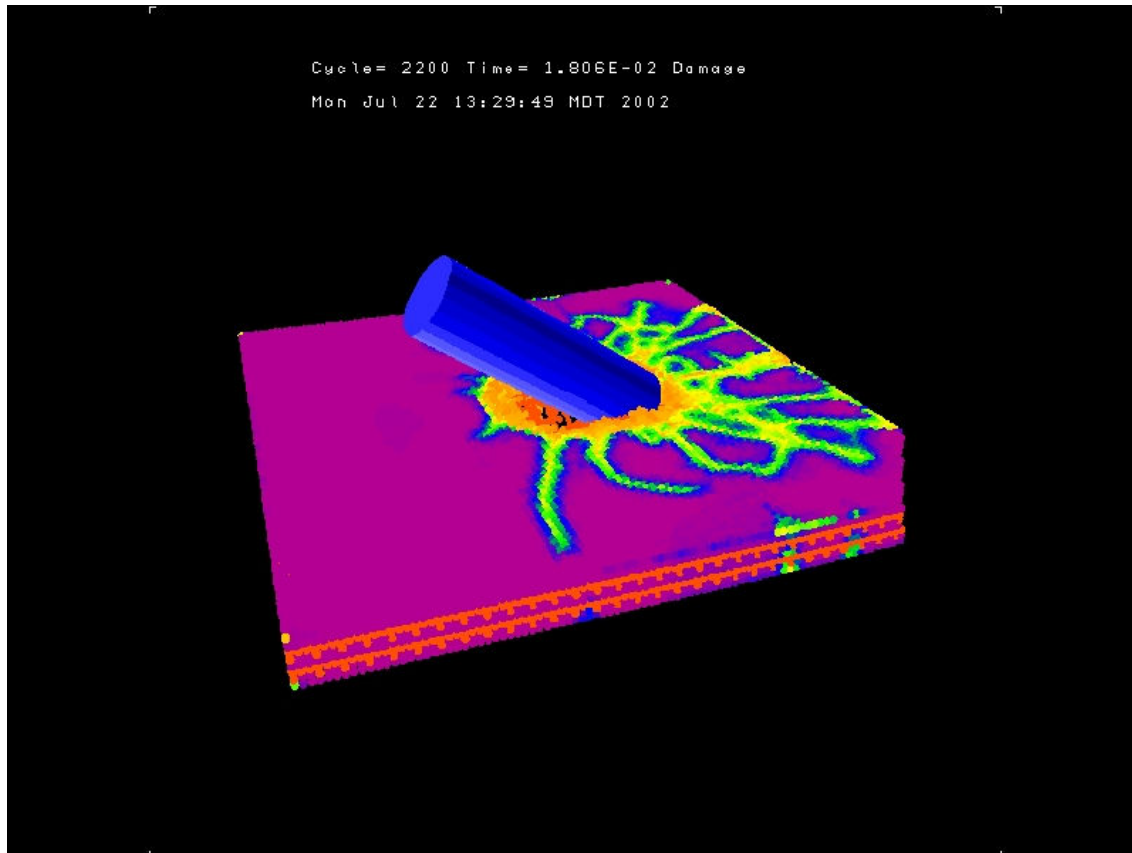
Entry crater

Exit crater

(Colors are included for visualization purposes only)

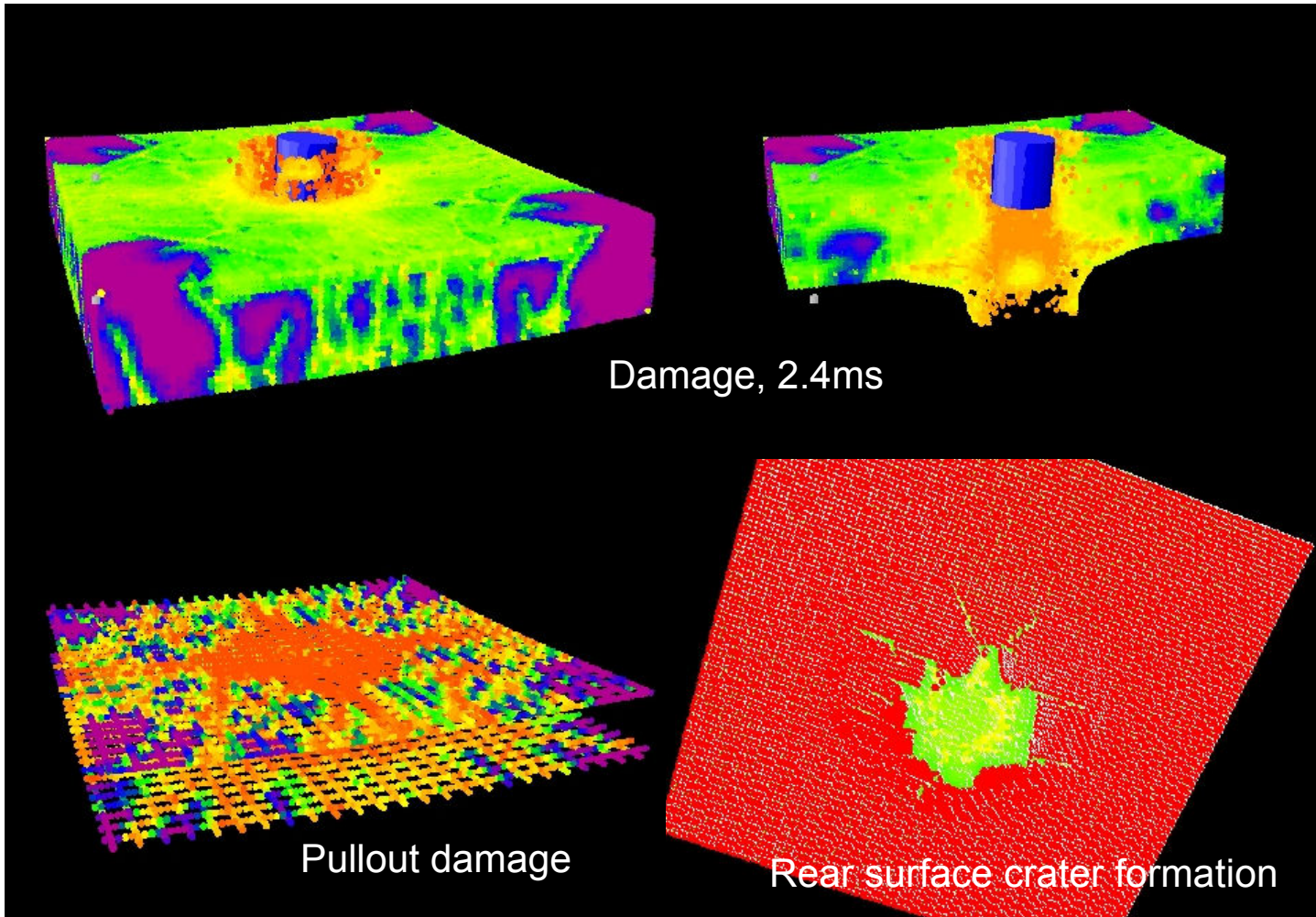


## Perforation: Cracks in a target due to oblique impact



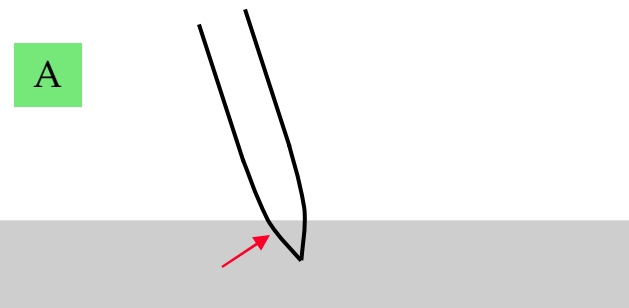


## Perforation: Explicit model of concrete reinforcement

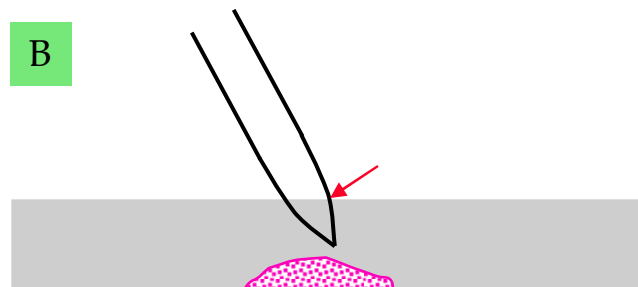




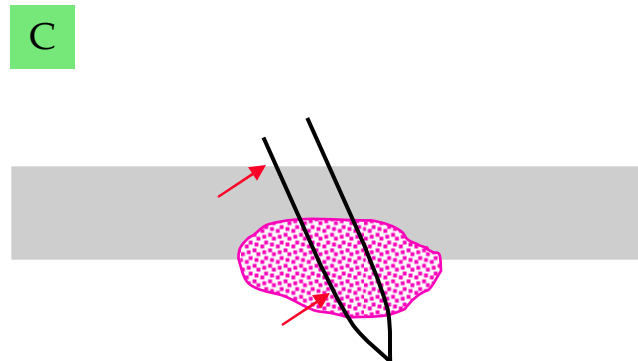
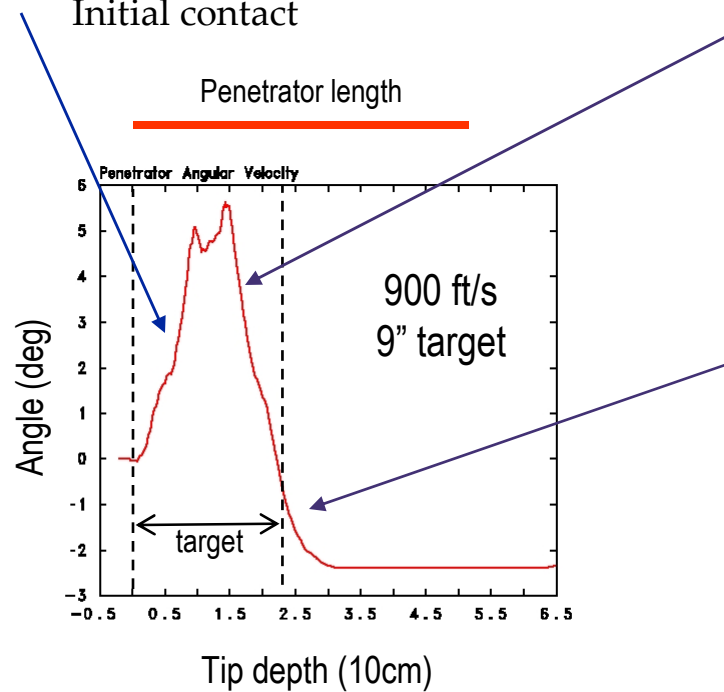
## Perforation: Forces that affect projectile rotation



Initial contact



Target is weaker below the impact point

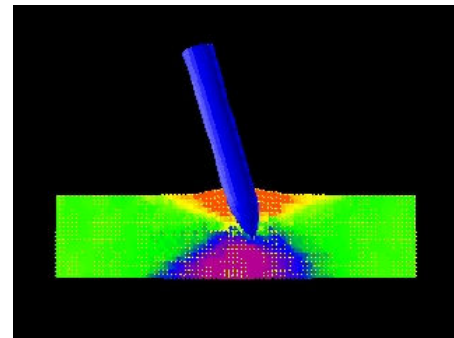
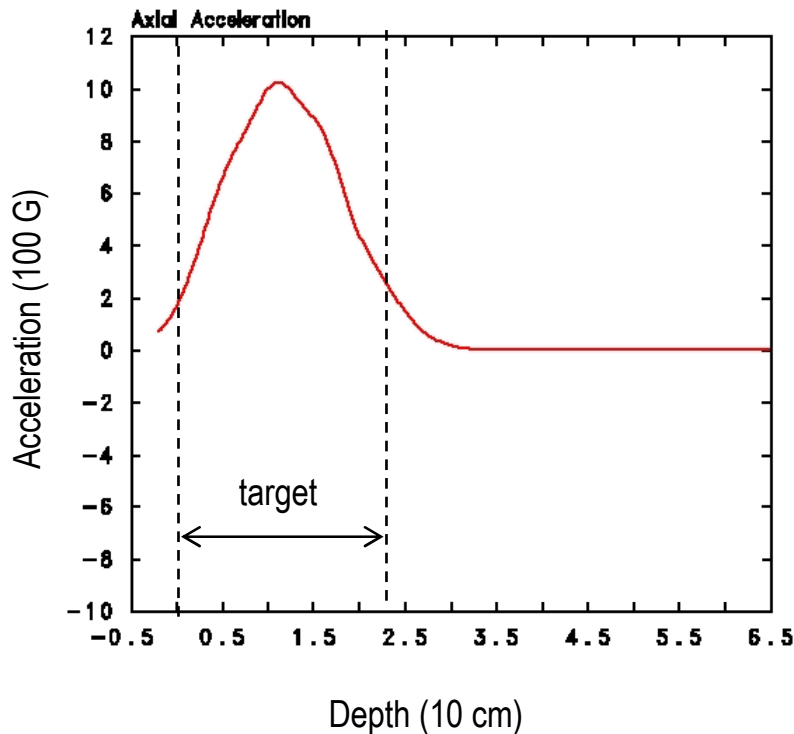


Tail slap + interaction with debris  
reverses the direction of rotation

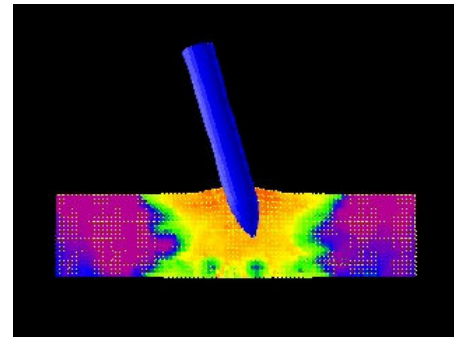


## Perforation of concrete: 900 ft/s into 9" target

- Peak axial acceleration occurs with nose tip is about halfway through the target.



z-velocity at time of peak axial acceleration

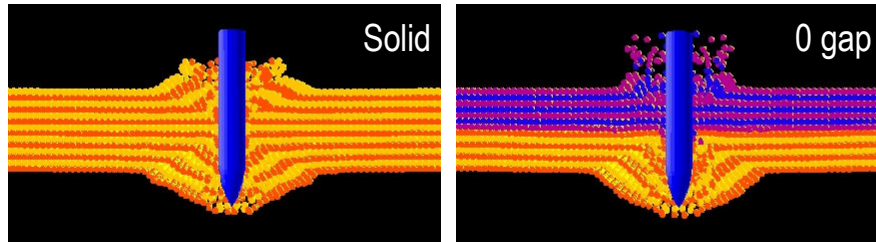


Damage at time of peak axial acceleration

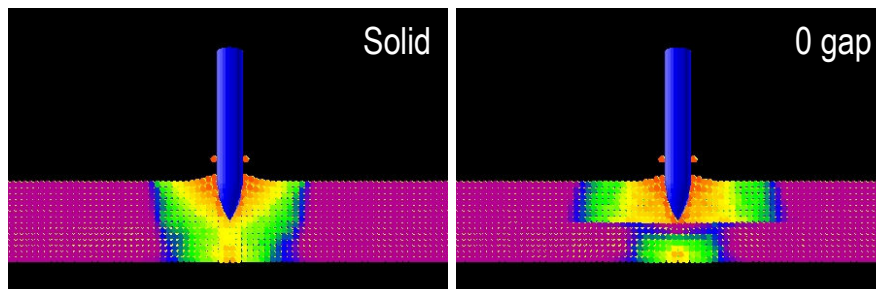


## Perforation: Solid vs. 2-panel target with 0mm gap

Crater shapes end up looking similar, however...

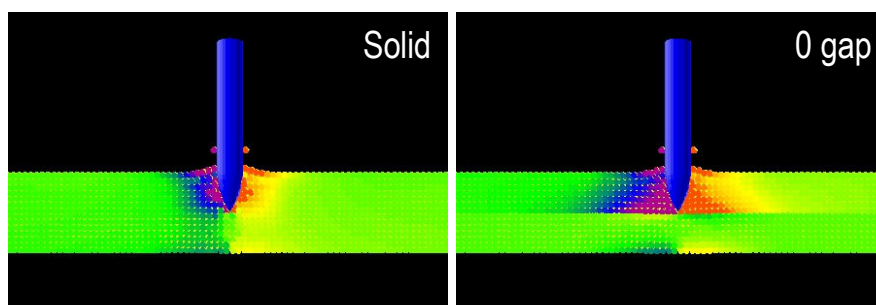


Cracks cannot propagate directly between panels.



Colors indicate damage (0.45 ms)

2-panel target shows less confinement near penetrator nose due to sliding at interface.



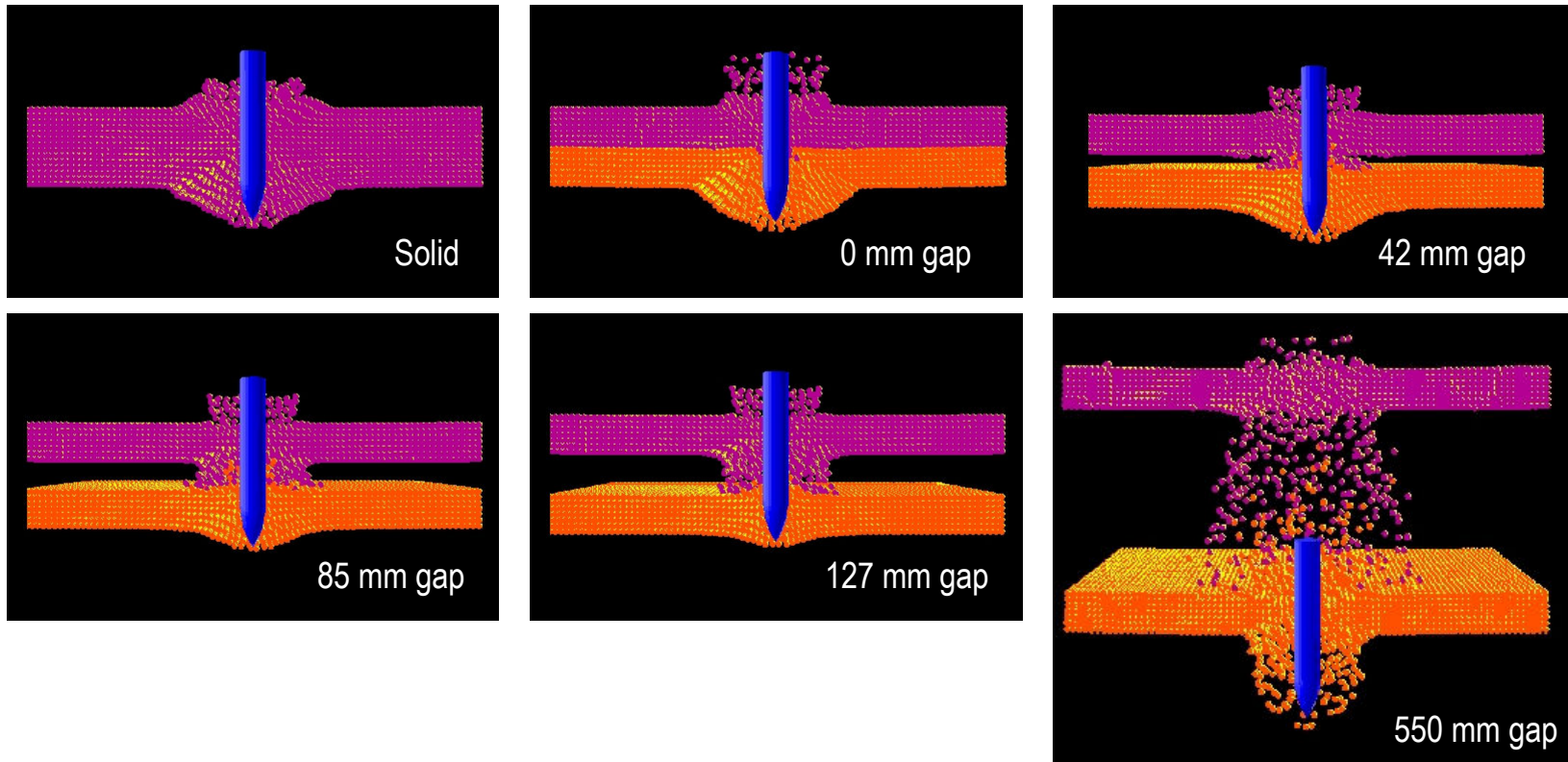
Colors indicate  $x$  component of displacement (0.45 ms)

→  $x$



## Perforation: Effect of a gap between 2 panels

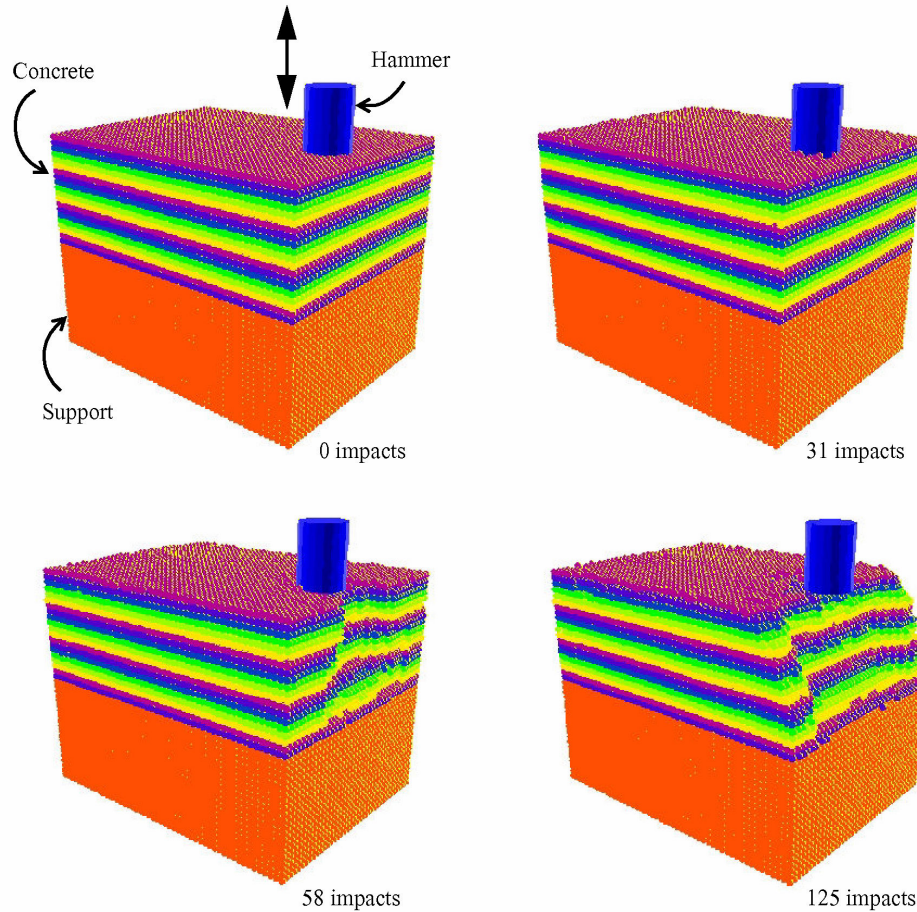
- How does the separation between concrete targets affect penetrator acceleration?





## Damage accumulation from multiple impacts

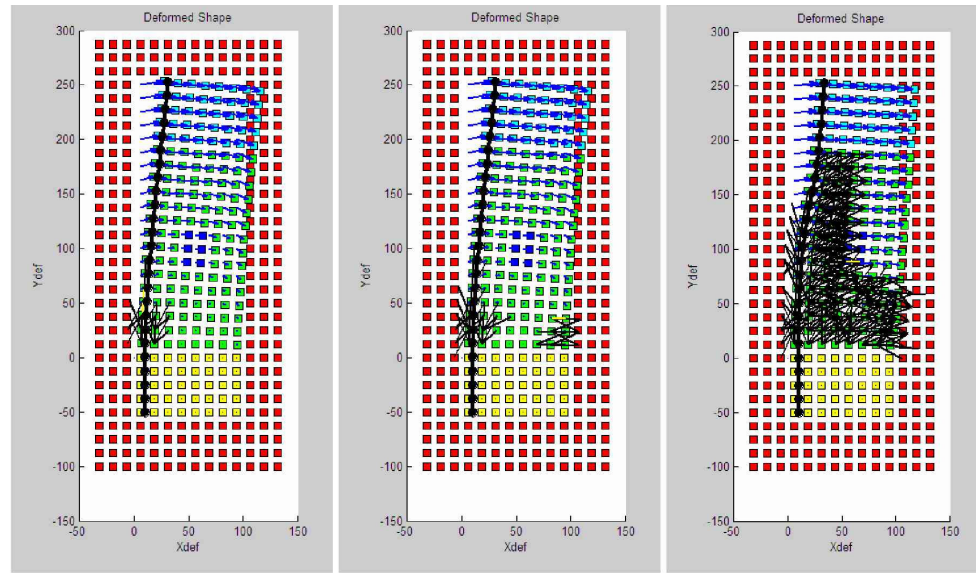
- Each successive impact breaks more bonds internally.
- These coalesce into large cracks.





# Degradation of elastic properties due to damage

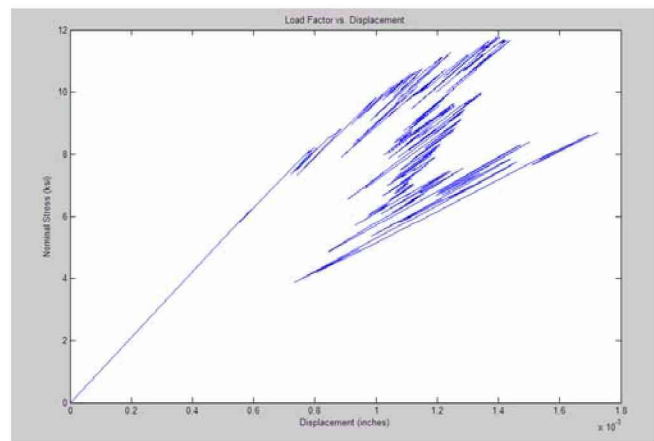
- Cantilevered concrete beam with single rebar  
(W. Gerstle, SMIRT-18)



(a) 25 links broken

(b) 50 links broken

(c) 400 links broken

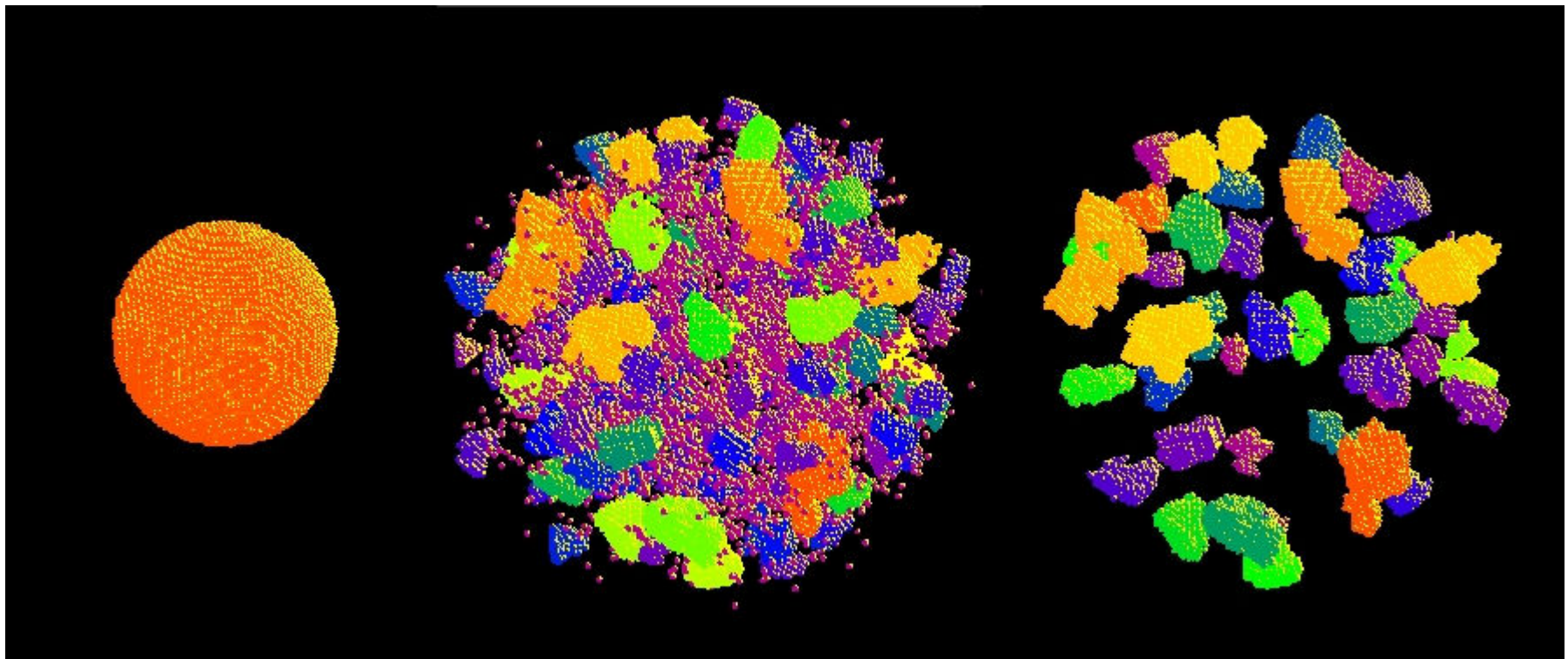


(d) Load versus load-point displacement



## Fragmentation: Brittle sphere expansion

- Uniform initial strain rate  $250\text{ s}^{-1}$ .



Initial

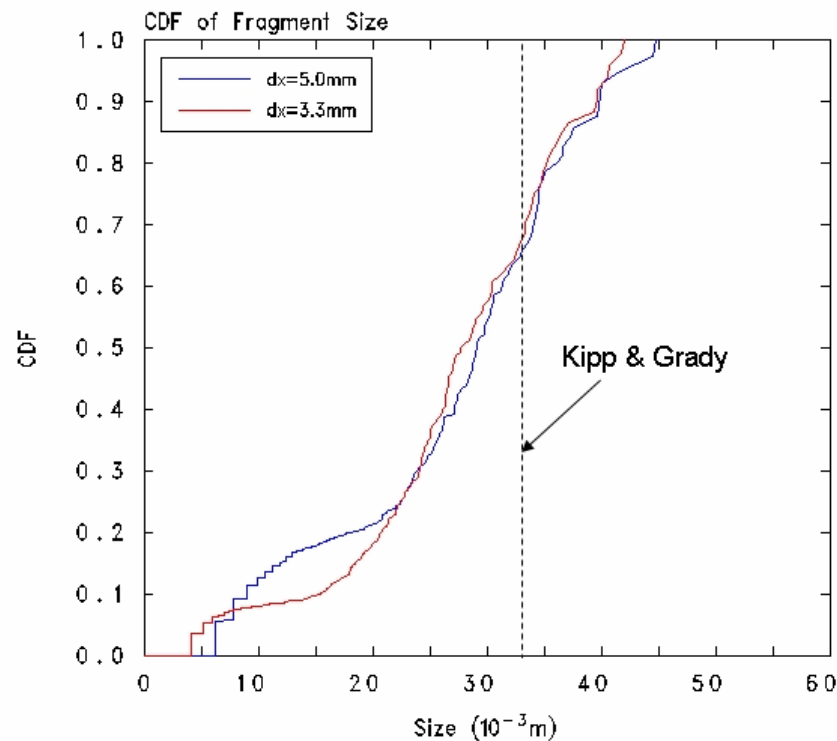
All fragments

Largest fragments



## Fragmentation: Brittle sphere expansion, ctd.

- Cumulative distribution function of fragment size.
  - Fragment size from Kipp-Grady equation is also shown.

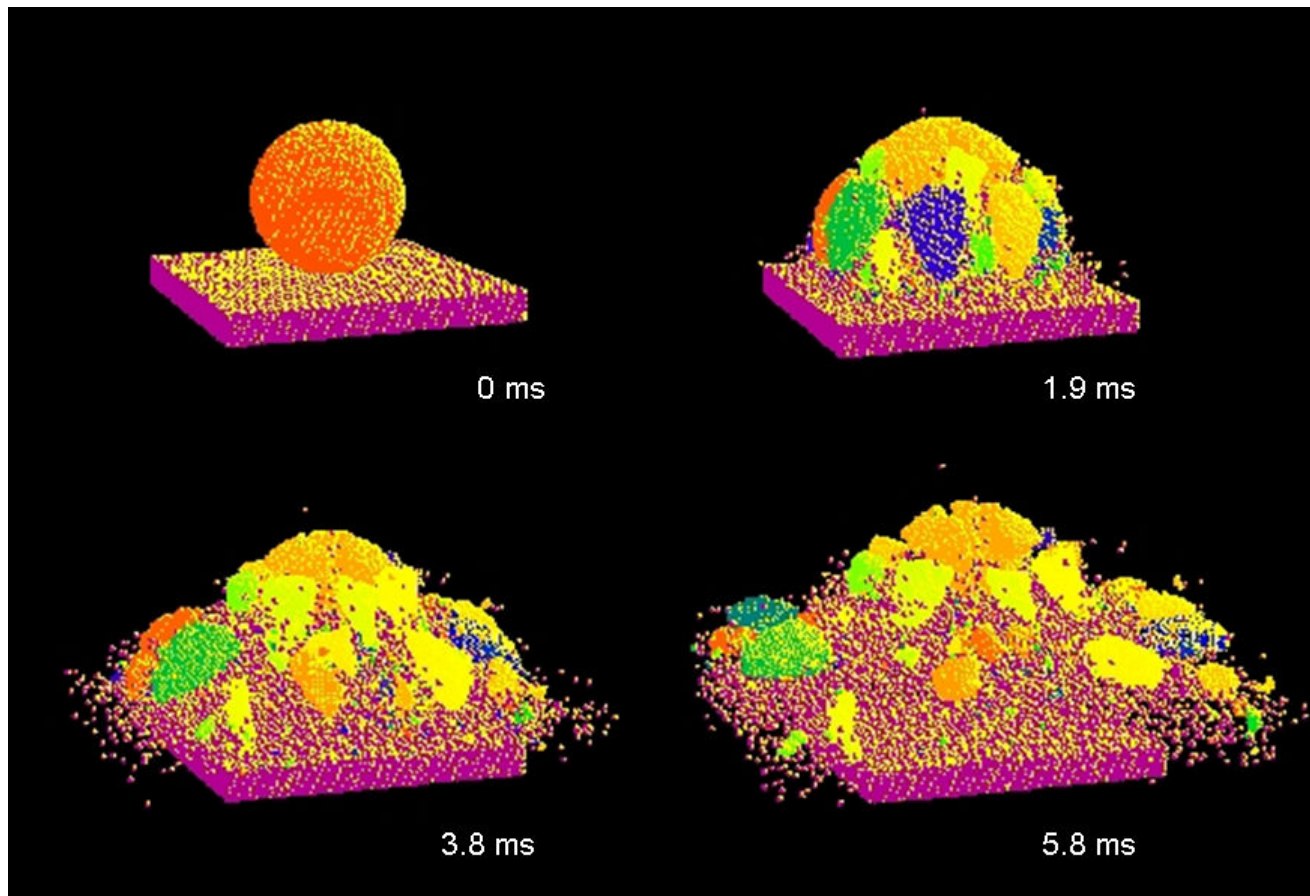




## Fragmentation: Concrete sphere drop

---

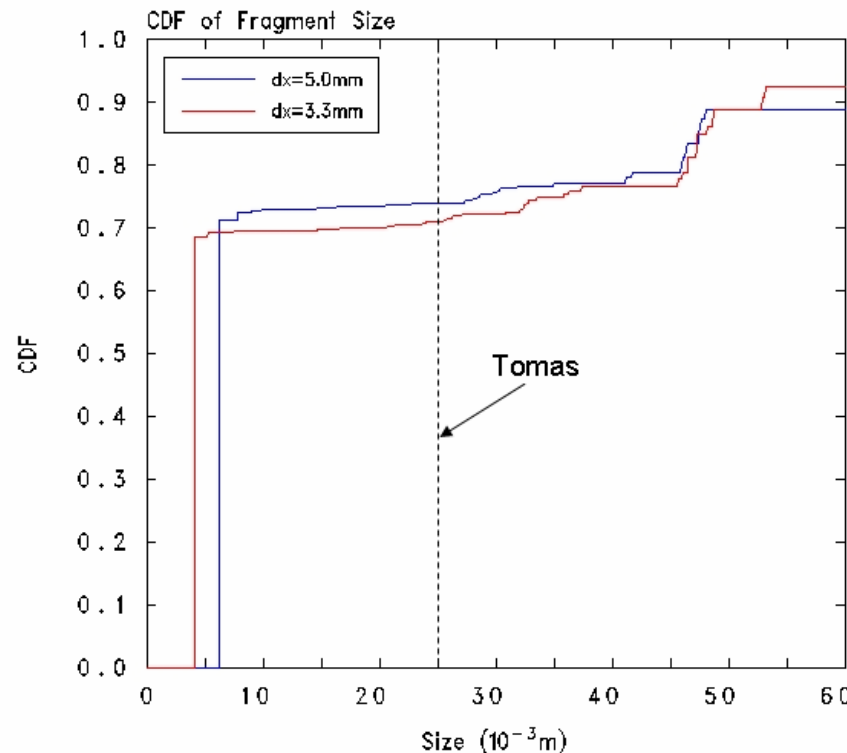
- 15cm diameter concrete sphere against a rigid plate, 32.4 m/s.





## Fragmentation: Concrete sphere drop, ctd.

- Cumulative distribution function of fragment size (for 2 grid spacings):
  - Also shows measured mean fragment size\*

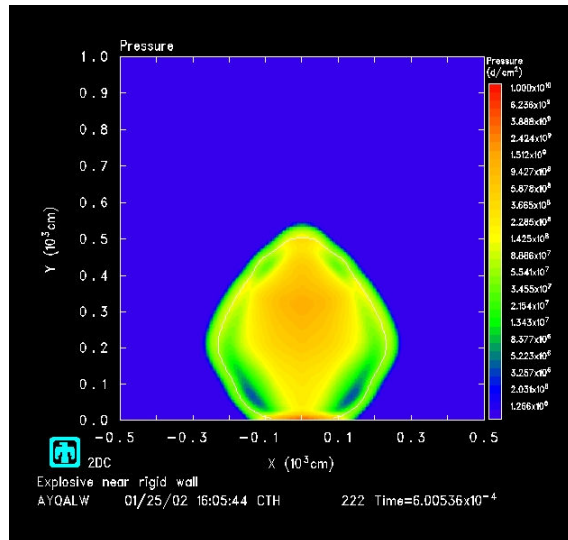


\*J. Tomas et. al., *Powder Technology* **105** (1999) 39-51.

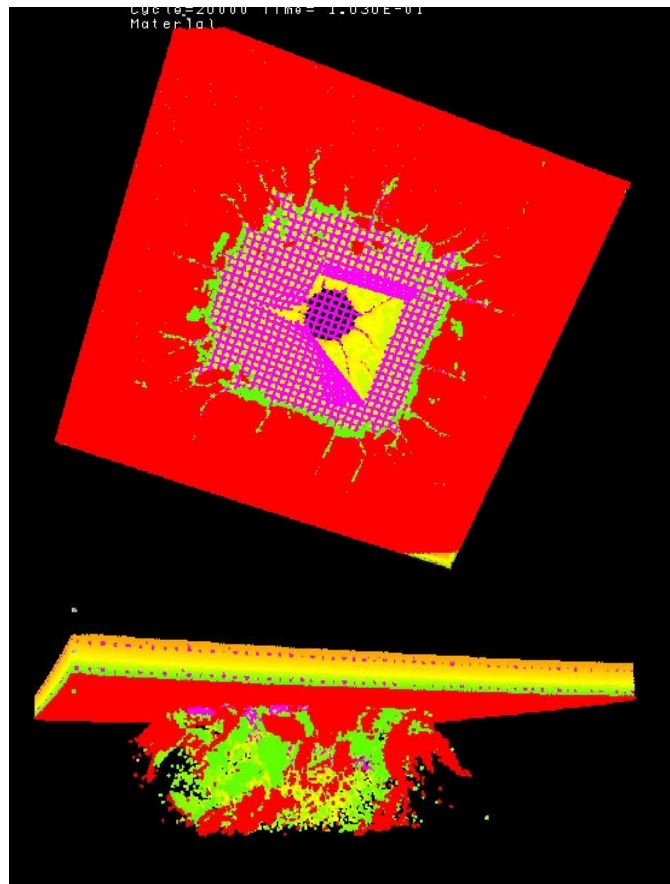


## Air blast effects

- Air blast loading on a reinforced concrete panel is supplied by the CTH code.



Air blast pressure field (from CTH)

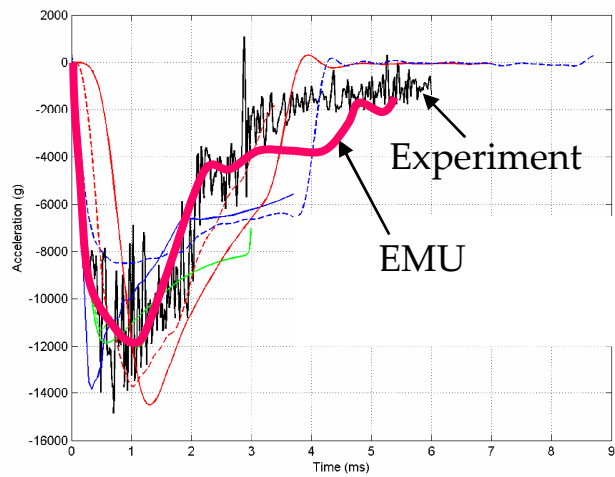


Panel response (from EMU)

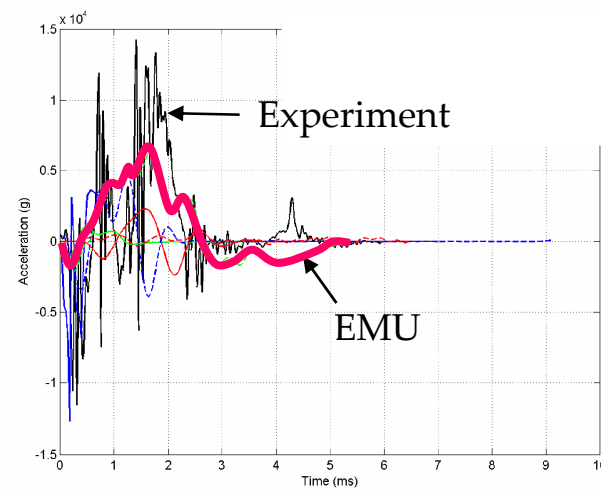


# Penetration benchmarking (DoD/DOE MOU): Genuine predictions

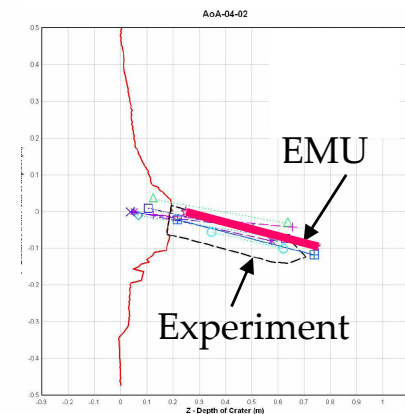
- Purpose: to exercise computational models in a predictive mode:
  - Model results are submitted before test data is released.
- 13kg steel penetrator into quality-controlled concrete targets.
  - On-board accelerometers both fore and aft.



Axial acceleration



Lateral acceleration



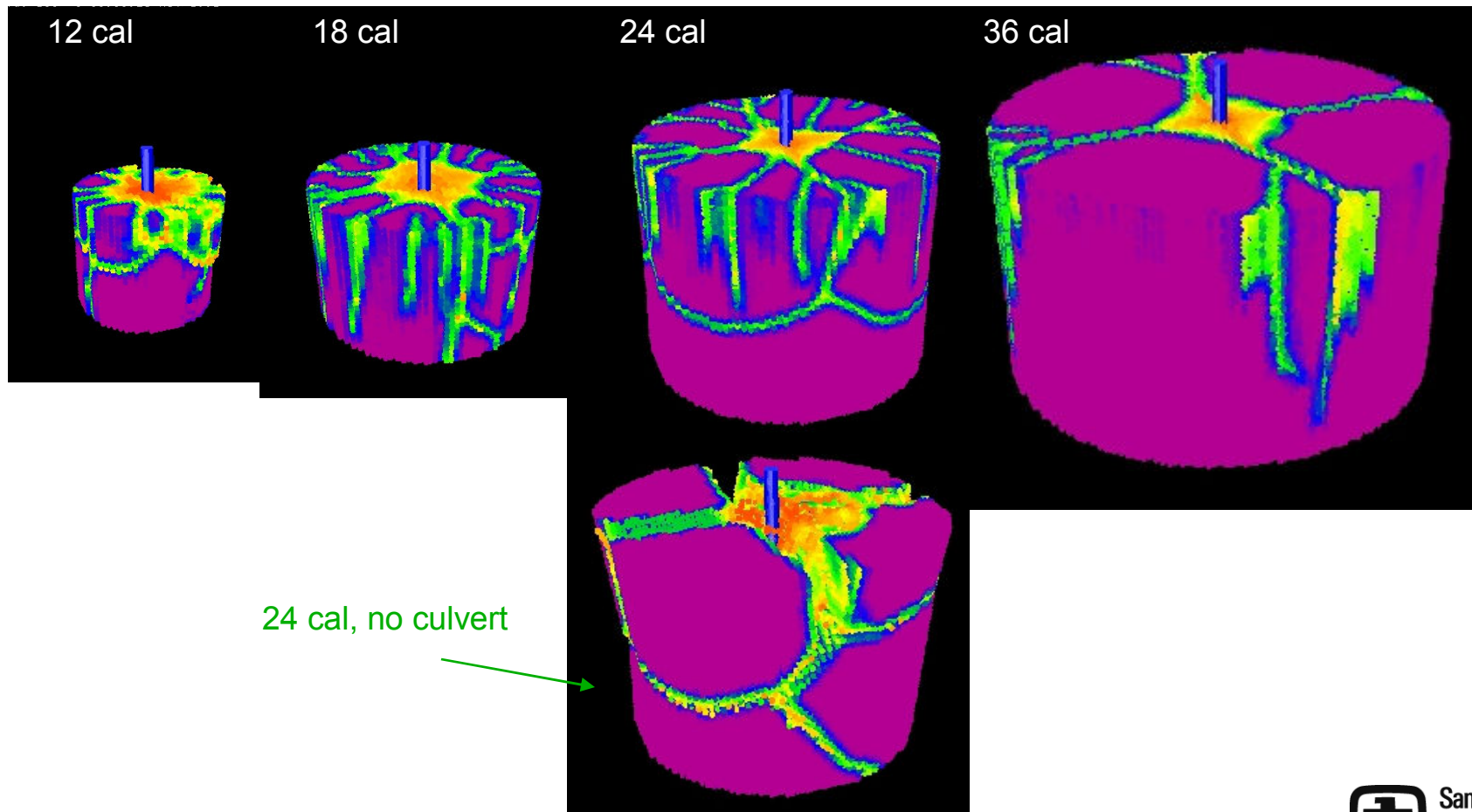
Rest position

*Unlabeled curves show other codes' predictions.*



## Penetration: Target diameter effect study

Cut-away views show only the target material deeper than 0.43m from the top surface.



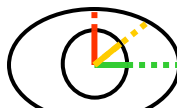


## Current research: Mathematics of a more general theory

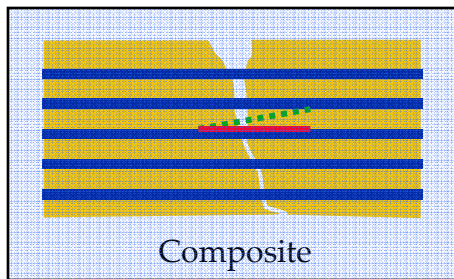
- **Peridynamic states**

- Mathematical generalization of the theory takes it far beyond what can be modeled with pair interactions.

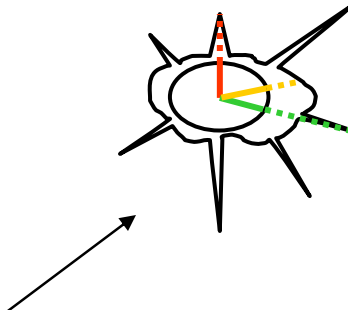
**Stress tensor (classical):**  
• 6 “degrees of freedom”.



$$\sigma = \begin{bmatrix} \sigma_{11} & \sigma_{12} & \sigma_{13} \\ \sigma_{21} & \sigma_{22} & \sigma_{23} \\ \sigma_{13} & \sigma_{23} & \sigma_{33} \end{bmatrix}$$



**Force state (peridynamic):**  
• Infinite “degrees of freedom”.



$$f = \underline{T}(x' - x)$$

Can use  
conventional  
material models.



## Peridynamic states vs. FE: Elastic-plastic solid

- Direct comparison between a finite-element code and Emu with a conventional material model.
- Results by T. Warren:

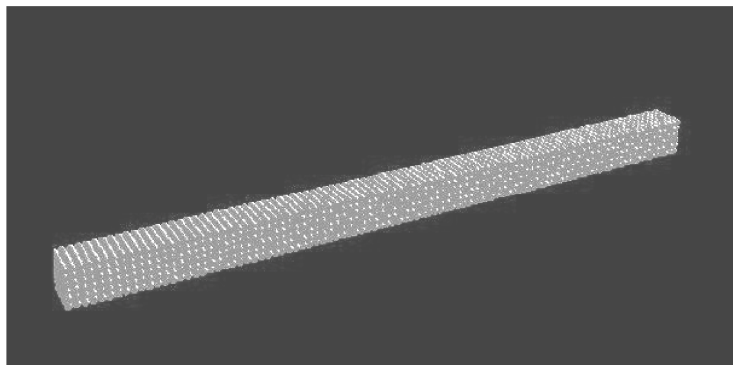


Figure 3. 3600 node discrete peridynamic lattice

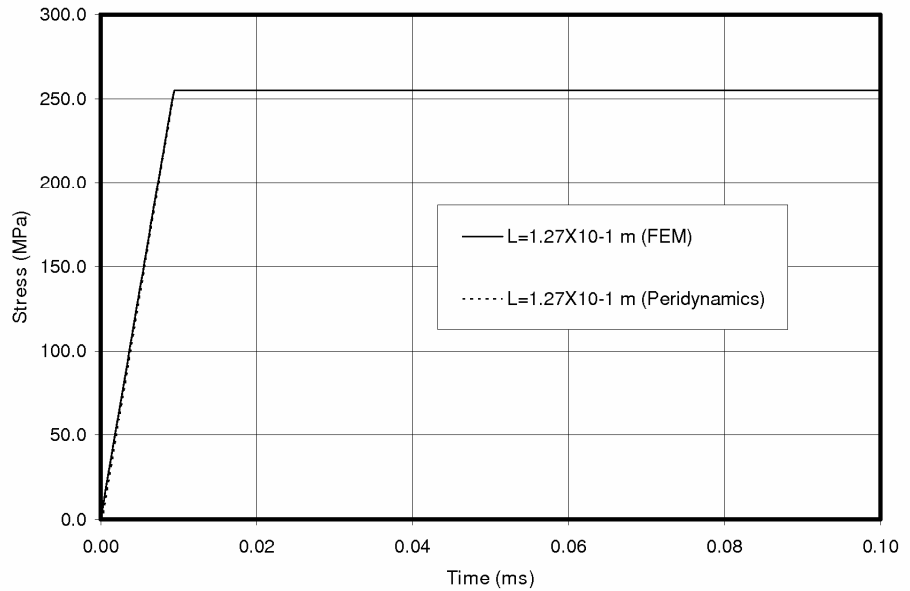


Figure 7. Stress in the bar at  $L=127$  mm using both Peridynamics and FEM



## Summary

---

- EMU fills a gap in the capabilities of conventional codes:
  - Ability to model discrete fractures.
  - Direct prediction of fragmentation.
- Current research areas related to concrete modeling:
  - Incorporation of conventional geological material models.
  - Rotational degrees of freedom.
- For more information and references: [www.sandia.gov/emu/emu.htm](http://www.sandia.gov/emu/emu.htm)